

Dear Reviewer #1,

Thank you for your review and the detailed comments. Below please find our point by point response to your suggestions and questions. The Reviewer's comments are in regular font and our response is in bold. **The line numbers correspond to the revised manuscript in "all mark up" view setting.**

### Response to Referee #1

In their study, the authors adapt a general mathematical method that was published by them earlier (2017) that can be used to determine and correct the biases related to the spatial aggregation of modeled, gridded evapotranspiration fields. The method is exemplarily applied for Switzerland, based on the GLEAM evapotranspiration model. I consider the contribution as innovative and as relevant for the field of hydrometeorological modeling and I recommend its publication after the following points were adequately addressed:

**We thank the reviewer for his/her interest in this work.**

#### General comments

Is it always that with higher resolution data models give more realistic estimates of ET? In the introduction you mainly address biases caused by rescaling of ET fields, but how does that rely to observations? Is there evidence in literature for the assumption that higher resolution data usually provides more realistic rates? You use GLEAM to prove your concept. But looking at the comparisons of true and estimated biases in Fig. S2 and S3, it seems that your approach does not work well for resolutions smaller than 0.25 (which is the target resolution of GLEAM). So maybe GLEAM is kind of optimized to this resolution and is not too realistic for higher ones? How would you explain the increased scatter between true and estimated biases for the 1/32 and 1/16 resolutions?

**First of all, it is important to remember that we are not comparing GLEAM with real-world measurements and therefore we cannot evaluate the realism of GLEAM at any resolution. We are not assuming that higher-resolution data is more realistic; instead, we use the higher-resolution estimates as a benchmark for synthetic experiments that examine how these ET estimates change with aggregation scale. As we note on lines 217-219, we use 500-m ET estimates (derived from GLEAM) as virtual "truth" and then see how these estimates, averaged over a range of larger scales, compare with GLEAM estimates of ET obtained from averages of temperature, net radiation, and soil moisture over those same larger scales.**

**We further looked into the point raised by the reviewer regarding the increased scatter between true and estimated biases for the 1/32 and 1/16 resolutions plots of figures S1 and S2. We noticed that due to a coding error, equations 10b, 13b, and 14b were not implemented correctly, meaning that the stress factor function was considered nonlinear in the full range of soil moisture and not only when soil moisture was between 0.1 and 0.6.**

**The stress factor function is nonlinear between volumetric soil moisture values of 0.1 and 0.6 as it is defined in GLEAM, and is equal to 0 or 1 outside this soil moisture range. Therefore the first and second derivatives of the ET function with regard to soil moisture are equal to 0 outside this range (eq10b, 13b, and 14b). Unfortunately we noticed that this point was overlooked in our original calculations in the code and the stress factor function was mistakenly considered as a nonlinear function for the entire range of soil moisture. We have**

now corrected this glitch and verified that the script is handling the 0.1 and 0.6 soil moisture conditions and the corresponding variability of soil moisture in this range correctly. The supplementary figures corresponding to estimated averaging error versus true averaging error for the two days also exhibit much less scatter than before. In fact, with this correction the  $R^2$  of the scatter plot of the 1/32 degree resolution increases to 0.91 on May 31<sup>st</sup> 2004 and 0.97 on July 21<sup>st</sup> 2004 after this correction. We will rerun the script and redraw all the figures in the revised manuscript.

After correcting this glitch, the estimated aggregation biases in Figures S1 and S2 were quite close to the one-to-one line for almost all the points, regardless of the resolution. This indicates that our method for predicting the aggregation bias generally works well. At the highest resolutions (smallest grid cells), however, there are a few cells that lie farther from the 1:1 line. These correspond to individual points in which the absolute values of ET are very small (snow-covered or glacierized landscapes), so even small prediction errors can appear as large percentage errors. But because these large percentage prediction errors are small in absolute terms, they mostly disappear when they are aggregated to larger grid cells. Thus the mean averaging error across Switzerland decreases sharply (almost exponentially) as the resolution increases.

Figure 2, 3, 4, S1, S2 and the related statements in the text have been changed throughout the manuscript.

Specific comments:

16: I would say that the drivers for droughts and heatwaves are precipitation, radiation, wind, temperature and soil moisture but not ET. Heatwaves occur because of the advection of warm and dry air. Droughts are caused by lacking precipitation. 42: Can you give a rough number (in percent) of typical deviations?

**We will correct this statement to: “Due to its feedbacks to large-scale hydrological processes and its impact on atmospheric dynamics, ET is one of the drivers of droughts and heatwaves”.**

Line 16 has changed to “ET is one of the drivers of droughts and heatwaves”.

With regard to the typical deviations, paragraph 2 and 3 of the introduction (Lines 47-70) report the direction and magnitude of these deviations according to a few studies.

140: Priestley-Taylor was already cited before in L 101.

**This citation is directly relevant to the PET formula and we found it is helpful to keep it where the equation is presented.**

167-173: You should cite your 2017 paper here again, is cited in the introduction but when I read the equations below a quick link to where they have been derived would be helping; also you should explain shortly the meaning of the variance and covariance terms here. They are only explained in L 246.

**We added the “Rouholahnejad Freund and Kirchner, 2017” paper as a reference (Line 172) and edited the explanation for equation 7 as: where  $\overline{ET}$  is the estimate of the true average of the nonlinear ET function over its variable inputs,  $\widehat{ET}$  is the ET function evaluated at its mean inputs, and the derivatives are understood to be evaluated at the mean values of the variables**

$(\overline{R_n}, \overline{w_w}, \overline{T})$  and multiplied by the corresponding variances and covariances among the finer-resolution input data.” (Lines 178-181)

177-179: Eq. 8 is not a derivative

We corrected the corresponding statement to make this point clearer: “For the specific case of the GLEAM model, the ET function is evaluated at its mean inputs ( $\overline{ET}$ ) and these derivatives are derived analytically from the ET function described by Eq. 6, directly yielding the following expressions:” (Lines 181-183)

179-188: Why was the interception term of Eq. 6 been skipped in the derivative calculations?

In GLEAM, interception loss is explicitly modelled according to Gash’s analytical model (Gash, 1979; Valente et al., 1997). Following this approach, the volume of water that evaporates from the canopy is estimated as a linear function of the daily rainfall using parameters that describe the canopy cover, canopy storage, and mean rainfall and evaporation rate during saturated canopy conditions.

Because the interception loss in GLEAM is a linear function of amount of rainfall necessary to saturate the canopy, it has negligible effects on the aggregation bias.

We added a statement to explain this point (Lines 197-199):

“Note that the interception term in equation 6 is dropped out from the derivatives as the interception loss in GLEAM is a linear function of amount of rainfall necessary to saturate the canopy and therefore has negligible effect when averaged.”

221-230: What algorithm was used for averaging?

-These are pure arithmetic averages (sum of values divided by number of values).

271-280: Are there dates where other variables than soil moisture have an increased impact?

The terms have different positive and negative contributions (increasing or decreasing effects on total bias) on the two days, with some of the variance and covariance terms being negative or positive. For example, the Rn and SM covariance term on May 31<sup>st</sup> 2004 is slightly negative (-0.53) but this same term is slightly positive on July 21<sup>st</sup> 2004 (0.88).

On most of the days of the year 2004, the soil moisture variance term is the dominant driver of the aggregation bias. However, there are some days in which other factors such as the T and Rn covariance term is the dominant factor (e.g, on days 285 and 297 of the year 2004, the T and Rn covariance term constitutes 74.5 % and 90.2 % of the aggregation bias).

309, 390, 391: The section references seem to be broken.

Thanks for pointing this out. We will revise the section numbers.

Fig. S2a) / S3a), please put the 6 maps into two rows, the color key numbers are hard to read

**We will do that.**

We redraw Figures S2a and S3a as requested (supplementary material, Figures S2 and S3)

References: unify format, many DOIs are missing, some are printed as links, some have no preceding "DOI" (please stick to HESS typesetting rules); Use en-dash for page ranges instead of simple dash

**We will do that.**

Line 468-561 are revised.

522: "Uber" -> "Über"

**We will revise "Uber" to "Über"**

"Uber" revised to "Über" (Line 552)

Minor:

15: feedbacks -> feedback 124: please change to "I is interception loss" or "I are interception losses" 367: two times "These biases can" maybe replace by "and"

**We will revise these points.**

Line 127 "interception losses" revised to "interception loss"

Lines 378-380 are revised to:

**"These biases can** be much larger for individual days (Figs. S2 and S3) **and potentially** have substantial consequences for water and energy flux estimates in land surface models and consequently for temperature predictions in coupled models."

Dear Reviewer #2,

Thank you for your review and the detailed comments. Following please find our point by point response to your suggestions and questions. The Reviewer's comments are in regular font and our response is in bold.

**The line numbers correspond to the revised manuscript in "all mark up" view setting.**

### **Response to Referee #2**

In this paper, the authors quantified and corrected the aggregation bias resulting from spatial heterogeneity in evapotranspiration (ET) estimates in a land evaporation model using the second-order Taylor expansions mathematical framework, an approach published by the authors previously in 2017. The GLEAM land surface model was chosen as its governing equations for calculating ET (Priestley-Taylor method) were amenable to analytical instead of numerical solutions and Switzerland was selected as the study area where high-resolution data (500m) on the ET drivers are available. This work is interesting and has important implications for Earth System Models. It can be accepted after several comments are addressed.

**We thank the reviewer for his/her interest in this work.**

General comments

In Figures 3 and 4, the graph for 1/32 degree seems missing. Moreover, Figures S2 and S3 (two selected days) indicate that the result shown in graph (1/32 degree) is not as good as other coarser resolutions, what is the possible reason for this?

**We looked into the point raised by the reviewer regarding the increased scatter between true and estimated biases for the 1/32 resolution plots of figures S1 and S2. We noticed that due to a coding error, equations 10b, 13b, and 14b were not implemented correctly, meaning that the stress factor function was considered nonlinear in the full range of soil moisture and not only when soil moisture is between 0.1 and 0.6.**

**The stress factor function is nonlinear between volumetric soil moisture values of 0.1 and 0.6 as it is defined in GLEAM, and is equal to 0 or 1 outside this soil moisture range. Therefore the first and second derivatives of ET function with regard to soil moisture are equal to 0 (eq10b, 13b, and 14b). Unfortunately we noticed that this point was overlooked in our original calculations in the code and the stress factor function was mistakenly considered as a nonlinear function for the entire range of soil moisture. We have now corrected this glitch and verified that script is handling the 0.1 and 0.6 soil moisture conditions and the corresponding variability of soil moisture in this range correctly. The supplementary figures corresponding to estimated averaging error versus true averaging error for the two days also exhibit much less scatter than before. In fact, with this correction the  $R^2$  of the scatter plot of the 1/32 degree resolution increases to 0.91 on May 31<sup>st</sup> 2004 and 0.97 on July 21<sup>st</sup> 2004 after this correction. We will rerun the script and redraw all the figures in the revised manuscript.**

**After correcting for this mistake, the estimated aggregation biases in Figures S1 and S2, were quite close to the one-to-one line for almost all the points, regardless of the resolution. This**

indicates that our method for predicting the aggregation bias generally works well. At the highest resolutions (smallest grid cells), however, there are a few cells that lie farther from the 1:1 line. These correspond to individual points in which the absolute values of ET are very small (snow-covered or glacierized landscapes), so even small prediction errors can appear as large percentage errors. But because these large percentage prediction errors are small in absolute terms, they mostly disappear when they are aggregated to larger grid cells. Thus the mean averaging error across Switzerland decreases sharply (almost exponentially) as the resolution increases.

Figure 2, 3, 4, S1, S2 and the related statements in the text have been changed throughout the manuscript.

The soil moisture plotted in Figure 1(B), S2(a) and S3(a) stands for the volumetric soil moisture (should be smaller than soil porosity) or soil moisture saturation (i.e. volumetric soil moisture/soil porosity, ranging from 0 and 1)? In addition, because spatial heterogeneity in soil moisture is found as the dominant driver of aggregation bias in ET estimates, perhaps the authors can provide the corresponding spatial distribution graph of soil moisture across different grid scales by averaging the 500m soil moisture in the supporting information.

**We will add the figure to the supplementary material**

Figure 1(B), S2(a) and S3(a) show volumetric soil moisture ranging from 0 to 1. The spatial distribution of soil moisture averages at several grid scales for the two randomly selected days are now added to the supplementary information (Figures S5 and S6).

Specific comments

Lines 58-61, it will be much clearer to the readers if the authors cite separately which literature found 'increases in average ET' and which literature reported 'decreases in grid-cell average ET'.

**We will cite the literature which reported decreases or increases in average ET separately in the revised manuscript.**

Line 59-63 are revised to:

"Several studies have reported increases in average evapotranspiration (ET) (e.g., Kuo et al., 1999; Boone and Wetzal, 1998; Hong et al., 2009; McCabe and Wood, 2006; El Maayar and Chen, 2006), and at least one has reported decreases in grid-cell average ET (Ershadi et al., 2013), as model grids are coarsened and less spatial heterogeneity is accounted for."

Line 117, 0.25-degree spatial resolution (i.e. corresponding to what kilometers?).

**0.25 degrees is about 27.6 km in the north-south direction and 18.9 km in the east-west direction at the latitude of Switzerland.**

Line 156 and Line 174, compared equation (6) and (7), the interception term (containing information about precipitation) is gone, why? Especially considering that this interception term is important as shown in Figure 1(E) and 1(F) as well as Figures S2(a) and S3(a).

**In GLEAM, interception loss is explicitly modelled according to Gash’s analytical model (Gash, 1979; Valente et al., 1997). Following this approach, the volume of water that evaporates from the canopy is estimated as a linear function of the daily rainfall using parameters that describe the canopy cover, canopy storage, and mean rainfall and evaporation rate during saturated canopy conditions.**

**Because the interception loss in GLEAM is a linear function of amount of rainfall necessary to saturate the canopy, it has negligible effects on the aggregation bias.**

**We added a statement to explain this point (Lines 197-199): “Note that the interception term in equation 6 is dropped out from the derivatives as the interception loss in GLEAM is a linear function of amount of rainfall necessary to saturate the canopy and therefore has negligible effect when averaged.”**

Lines 222-224, how did the authors conduct the “average” algorithm?

**These are pure arithmetic averages (sum of values divided by number of values).**

Table 1, the two example days showed that variance of soil moisture is the dominant driver of aggregation bias in ET estimates, is this true for all the other days?

**We re-ran the analysis for the entire Switzerland for every day of the year 2004. In most of the days of the year 2004, soil moisture variance term is the dominant driver of the aggregation bias. However, there are some days in which other factors such as the T and Rn covariance term is the dominant factor (e.g, days 285 and 297 of the year 2004, the T and Rn covariance term constitutes 74.5 % and 90.2 % of the aggregation bias).**

Technical corrections

Lines 309, 390, 381, section 5.1 and 5.2 is typo.

**OK.**

1 **Averaging over spatiotemporal heterogeneity substantially biases evapotranspiration rates in a mechanistic**  
2 **large-scale land evaporation model**

3 Elham Rouholahnejad Freund<sup>1,2,3</sup>, Massimiliano Zappa<sup>4</sup>, James W. Kirchner<sup>3,4,5</sup>

4

5 <sup>1</sup>Laboratory of Hydrology and Water Management, Ghent University, Ghent, Belgium

6 <sup>2</sup>Chair of Hydrology, Faculty of Environment and Natural Resources, University of Freiburg, Freiburg, Germany

7 <sup>3</sup>Department of Environmental Systems Science, ETH Zurich, CH-8092 Zürich, Switzerland

8 <sup>4</sup>Swiss Federal Research Institute WSL, CH-8903 Birmensdorf, Switzerland

9 <sup>5</sup>Department of Earth and Planetary Science, University of California, Berkeley, CA 94720 USA

10

11 Correspondence to: Elham Rouholahnejad Freund, elham.rouholahnejad@gmail.com

12

13 **Abstract**

14 Evapotranspiration (ET) influences land-climate interactions, regulates the hydrological cycle, and contributes  
15 to the Earth's energy balance. Due to its feedbacks to large-scale hydrological processes and its impact on  
16 atmospheric dynamics, ET is one of the a-key drivers of droughts and heatwaves. Existing land surface models  
17 differ substantially, both in their estimates of current ET fluxes and in their projections of how ET will evolve in  
18 the future. Any bias in estimated ET fluxes will affect the partitioning between sensible and latent heat, and  
19 thus alter model predictions of temperature and precipitation. One potential source of bias is the so-called  
20 "aggregation bias" that arises whenever nonlinear processes, such as those that regulate ET fluxes, are  
21 modeled using averages of heterogeneous inputs. Here we demonstrate a general mathematical approach to  
22 quantifying and correcting for this aggregation bias, using the GLEAM land evaporation model as a relatively  
23 simple example. We demonstrate that this aggregation bias can lead to substantial overestimates in ET fluxes  
24 in a typical large-scale land surface model when sub-grid heterogeneities in land surface properties are  
25 averaged out. Using Switzerland as a test case, we examine the scale-dependence of this aggregation bias and  
26 show that it can lead to an average overestimation of daily ET fluxes by as much as 2410% averaged over across  
27 the whole country (calculated as the median of the daily bias over the growing season). We show how our  
28 approach can be used to identify the dominant drivers of aggregation bias, and to estimate sub-grid closure  
29 relationships that can correct for aggregation biases in ET estimates, without explicitly representing sub-grid  
30 heterogeneities in large-scale land surface models.

31 **Plain Language Summary**

32 Evapotranspiration (ET) is the largest flux from the land to the atmosphere and thus contributes to Earth's  
33 energy and water balance. Due to its impact on atmospheric dynamics, ET is a key driver of droughts and  
34 heatwaves. In this paper, we demonstrate how averaging over land surface heterogeneity contributes to  
35 substantial overestimates of ET fluxes. We also demonstrate how one can correct for the effects of small-scale  
36 heterogeneity without explicitly representing it in land surface models.



37

## 38 1. Introduction

39 Earth's surface and subsurface are characterized by spatial heterogeneity spanning wide ranges of scales,  
40 including scales that cannot be explicitly resolved by large-scale Earth System Models (ESMs), which are  
41 typically run at resolutions of 10-100 kilometers. Averaging over this finer-scale heterogeneity can bias model  
42 estimates of water and energy fluxes and hence alter future temperature predictions. Earth system model  
43 estimates of global terrestrial evaporation differ substantially from atmospheric reanalyses based on in-situ  
44 and satellite remote sensing observations (Mueller et al., 2013), but it is unclear how much of these  
45 differences could be attributed to errors in capturing sub-grid heterogeneity.

46

47 Several recent studies (e.g., Fan et al., 2019; Shrestha et al., 2018) have emphasized the need ~~to account to~~  
48 account for land surface heterogeneity in large-scale ESMs. Despite recent community efforts in refining ESMs'  
49 spatial resolution (Huang et al., 2016; Rauscher et al., 2010; Ringler et al., 2008; Skamarock et al., 2012;  
50 Zarzycki et al., 2014), the grid resolution of present-day ESMs is still too coarse to explicitly capture important  
51 effects of surface heterogeneity. Whether the solution lies in hyper-resolution large-scale land surface  
52 modeling remains an open question, because heterogeneities that are important to land-atmosphere fluxes  
53 will not be fully resolved even at scales of 100 m (Beven and Cloke, 2012).

54

55 The effects of aggregating over spatial heterogeneity in land surface models have been assessed using several  
56 approaches. Most of these approaches compare grid-cell-averaged energy and water fluxes with flux estimates  
57 for finer-resolution grids, or for grid cells that are subdivided into mosaics of several surface types which  
58 separately exchange momentum, energy, and water vapor with the overlying atmosphere (e.g., Giorgi, 1997).  
59 Several studies have reported increases in average evapotranspiration (ET) (e.g., Kuo et al., 1999; Boone and  
60 Wetzel, 1998; Hong et al., 2009; McCabe and Wood, 2006; Ershadi 2013; El Maayar and Chen, 2006), and at  
61 least one has reported decreases in grid-cell average ET (Ershadi et al., 2013), as model grids are coarsened  
62 and less spatial heterogeneity is accounted for (~~e.g., Kuo et al., 1999; Boone and Wetzel, 1998; Hong et al.,~~  
63 ~~2009; McCabe and Wood, 2006; Ershadi 2013; El Maayar and Chen, 2006~~). Shrestha et al. (2018) studied the  
64 effects of horizontal grid resolution on ET partitioning in the TerrSysMP Earth system model and found that the  
65 aggregation of topography decreases average slope gradients and obscures small-scale convergence and  
66 divergence zones, directly impacting surface and subsurface flow. They observed 5 and 8 percent decreases in  
67 the transpiration/evapotranspiration ratio for a dry and a wet year, respectively, when their model grid cells  
68 were coarsened from 120 m to 960 m. All these studies calculate the effects of land surface heterogeneity on  
69 ET fluxes using numerical experiments that refine the model's spatial resolution, either directly or through the  
70 use of land-surface mosaics.

71

72 Quantifying the effect of sub-grid scale heterogeneity on grid-cell-averaged fluxes is especially important when  
73 highly nonlinear processes are involved. Regardless of scale, the main challenge is not to explicitly represent  
74 the heterogeneity in all its details, but instead to define an appropriate scale-dependent sub-grid closure

75 relationship that recognizes the important heterogeneities within the grid elements and the nonlinearities in  
76 the processes (Beven, 2006). Such a sub-grid closure scheme would capture the effects of sub-grid  
77 heterogeneity in large-scale land surface models without forcing them to run at finer spatial resolutions.

78

79 We have recently proposed a general theoretical framework, based on Taylor series expansions, that  
80 quantifies the "aggregation bias" that results from averaging over sub-grid heterogeneity when grid-cell-  
81 averaged ET is estimated (Rouholahnejad Freund and Kirchner, 2017; Rouholahnejad Freund et al., 2019). In  
82 contrast to the numerical experiments described above, this theoretical framework does not depend on a  
83 particular evapotranspiration model or grid scale. Our previous work demonstrated this framework using  
84 Budyko curves as a see-through "toy" model, leaving open the question of how strongly ET estimates would be  
85 affected by sub-grid heterogeneity in a more typical mechanistic evapotranspiration model. Here we use the  
86 mechanistic evapotranspiration model GLEAM to quantify how aggregation biases vary across a range of  
87 scales, using Switzerland as a case study. We show how our Taylor expansion framework can be used to  
88 quantify the sensitivity of ET fluxes to heterogeneity in their individual drivers. We further demonstrate how  
89 this framework can be used to estimate correction factors (i.e., sub-grid closure relationships) that account for  
90 the effects of sub-grid heterogeneity without explicitly modeling it, and show how these correction factors can  
91 be used to improve grid-scale ET estimates. Because our framework is not model-specific, the analysis  
92 presented here could also be applied to many other evapotranspiration algorithms.

93

## 94 **2. Methods and results**

### 95 **2.1. A common mechanistic framework for predicting evapotranspiration**

96 Most large-scale land surface models calculate ET as a function of available water and energy at daily time  
97 steps. They typically multiply an estimate of potential evapotranspiration (PET) by a conversion factor to  
98 calculate actual evapotranspiration. PET is generally understood as the maximum rate of evapotranspiration  
99 from a large area (to avoid the effect of local advection) covered completely and uniformly by actively growing  
100 vegetation with adequate moisture at all times (Brutseart, 1984). Models typically estimate PET using the  
101 Penman equation (Penman, 1948; intended for open water surfaces), the Penman-Monteith equation  
102 (Monteith, 1965, Monteith and Unsworth, 1990; intended for reference crop evapotranspiration by adding  
103 atmospheric transport processes and stomatal resistance to Penman's open water evaporation), or the  
104 Priestley-Taylor equation (Priestley and Taylor, 1972; intended for open water and water-saturated crops and  
105 grasslands). The conversion factor that is used to estimate ET from PET typically depends on plant physiology  
106 and on the water that is available for evaporation.

107

108 Here, we employ an ET algorithm that is used by several land surface models (i.e., Global Land-surface  
109 Evaporation: The Amsterdam Methodology (GLEAM); Miralles et al., 2011; Martens et al., 2017), in which  
110 actual ET is calculated as a fraction of PET. This fraction is expressed as a multiplicative factor, often called a  
111 stress factor, which ranges between 0 and 1 and thus limits ET rates. Under wet conditions, ET can equal PET  
112 (stress factor equals one) while under dry conditions, PET is multiplied by a stress factor smaller than one

113 depending on the degree of water stress. This approach is employed by the GLEAM model, among others.  
 114 GLEAM is a diagnostic satellite-data-driven method that is used to estimate global land evaporation fluxes.  
 115 GLEAM uses the Priestley-Taylor formula and remotely sensed datasets of radiation and temperature to  
 116 calculate PET. In GLEAM, actual ET is calculated by constraining PET estimates by a stress factor that is based  
 117 on estimates of root-zone soil moisture. The root zone soil moisture is derived from a multi-layer water  
 118 balance module that describes the infiltration of precipitation through the vertical soil profile. ET estimates  
 119 from GLEAM have been applied in many studies (e.g., Miralles et al., 2013; Miralles et al., 2014; Greve et al.,  
 120 2014; Jasechko et al., 2013). GLEAM operates on daily time steps at 0.25-degree spatial resolution. To the best  
 121 of our knowledge, there are no prior studies quantifying the aggregation bias in ET estimates from GLEAM or  
 122 other models with similar ET formulations.

123

124 GLEAM calculates ET as an explicit function of the stress factor and potential evaporation:

$$125 \quad ET = S \cdot PET + (1 - \beta) I, \quad (1)$$

126 where  $ET$  is actual evapotranspiration ( $\text{mm d}^{-1}$ ),  $S$  is the evaporative stress factor (-) that accounts for  
 127 environmental conditions that reduce actual ET relative to potential ET,  $I$  is interception losses ( $\text{mm d}^{-1}$ ), and  $\beta$   
 128 is a constant ( $\beta = 0.07$  – Gash and Stewart, 1977) that avoids double-counting of interception losses during  
 129 hours with wet canopy. The stress factor ( $S$ ) depends on the soil moisture conditions, and is parametrized  
 130 separately for tall canopy, short vegetation, and bare soil. GLEAM uses the following soil-moisture-based  
 131 parameterization to calculate the stress factor (Miralles et al., 2011; Martens et al., 2017):

$$132 \quad S = 1 - \left( \frac{w_c - w_w}{w_c - w_{wp}} \right)^2, \quad (2)$$

133 where  $S$  is the stress factor (-) for tall canopy,  $w_w$  is the volumetric soil moisture at any given time ( $\text{m}^3 \text{m}^{-3}$ ), and  
 134  $w_c$  and  $w_{wp}$  are the critical soil moisture level and soil moisture at wilting point. For soil moisture values below  
 135 the wilting point  $w_{wp}$ , the stress is maximal (stress factor equals 0), causing ET to sharply decline to zero. For  
 136 values above the critical moisture level  $w_c$ , there is no water stress (stress factor equals 1) and ET equals PET.  
 137 Between  $w_{wp}$  and  $w_c$  the stress increases as soil moisture decreases following a parabolic function (Eq. 2). In  
 138 the analysis presented below, we set the critical soil moisture level ( $w_c$ ) and soil moisture at wilting point  
 139 ( $w_{wp}$ ) to 0.6 and 0.1  $\text{m}^3 \text{m}^{-3}$  respectively. To simplify the analysis presented below, we have used the tall-  
 140 canopy stress factor (Eq. 2) for all of Switzerland, even though the short-canopy or bare-soil formulations may  
 141 be better suited to some locations.

142

143 GLEAM uses the Priestley-Taylor approach to calculate PET (Priestley and Taylor, 1972):

$$144 \quad PET = \frac{\alpha}{\lambda} \frac{\Delta}{\Delta + \gamma} (R_n - G), \quad (3)$$

145 where  $PET$  is potential evapotranspiration ( $\text{mm d}^{-1}$ ),  $\alpha$  is a dimensionless coefficient that parametrizes the  
 146 resistance to evaporation and is set to 0.8 for tall canopy in GLEAM (Miralles et al., 2011),  $\lambda = 2.26$  ( $\text{MJ kg}^{-1}$ ) is  
 147 the latent heat of vaporization,  $R_n$  is net radiation ( $\text{MJ m}^{-2} \text{d}^{-1}$ ),  $G$  is the ground heat flux, approximated as  
 148  $G = 0.05 R_n$  ( $\text{MJ m}^{-2} \text{d}^{-1}$ ) for tall canopy in GLEAM,  $T$  is temperature ( $^{\circ}\text{C}$ ), and  $\Delta$  is the slope of the

149 temperature/saturated vapor pressure curve ( $\text{kPa}^\circ\text{C}^{-1}$ ), which is functionally related to temperature (Tetens,  
150 1930; Murray, 1967; Stanghellini, 1987):

$$151 \quad \Delta = ae^{bT}, \quad (4)$$

152 where  $a = 0.04145$  ( $\text{kPa}^\circ\text{C}^{-1}$ ),  $b = 0.06088$  ( $^\circ\text{C}^{-1}$ ), and  $\gamma$  is the psychrometric constant ( $\text{kPa}^\circ\text{C}^{-1}$ ) which can be  
153 calculated as (Brunt, 1952):

$$154 \quad \gamma = \frac{C_{p_{air}} * P}{\lambda * MW_{ratio}}, \quad (5)$$

155 where  $C_{p_{air}} = 0.001013$  ( $\text{MJ kg}^{-1}\text{C}^{-1}$ ) is the specific heat of air at constant pressure,  $P = 101.3$  (KPa) is  
156 atmospheric pressure, and  $MW_{ratio} = 0.622$  (-) is the molecular weight ratio of  $\text{H}_2\text{O}/\text{air}$ . Substituting the  
157 aforementioned constants in Eq. 5 yields  $\gamma = 0.073$  ( $\text{kPa}^\circ\text{C}^{-1}$ ). Expanding Eq. 1 using Eqs. 2-5 yields the ET  
158 function as calculated by GLEAM:

$$159 \quad \begin{aligned} ET_{[mmd^{-1}]} &= \left[ -4w_w[m^3m^{-3}]^2 + 4.8w_w[m^3m^{-3}] - 0.44 \right] * \frac{\alpha_{[ ]}}{\lambda_{[MJ kg^{-1}]} * \Delta_{[kPa^\circ C^{-1}]} + \gamma_{[kPa^\circ C^{-1}]}} \\ &\quad * 0.95 * \frac{86400}{1000000} * R_n[w_m^{-2}] + (1 - \beta) I_{[mmd^{-1}]} \\ &= \left[ -4w_w^2 + 4.8w_w - 0.44 \right] * 0.02905 * \frac{a e^{bT}}{a e^{bT} + 0.073} R_n + (1 - 0.07) I_{[mmd^{-1}]} \end{aligned} \quad (6)$$

160

161 In the analysis below, we use [the GLEAM evapotranspiration algorithm](#) to demonstrate how aggregation biases  
162 can be estimated in land surface modeling schemes. We chose GLEAM because its governing equations are  
163 amenable to the analytical solutions derived below. Here we make no particular claim for the accuracy or  
164 validity of GLEAM as an evapotranspiration model, nor is our analysis intended to test this. Likewise our  
165 analysis should not be interpreted as implying that GLEAM is any more, or less, susceptible to aggregation bias  
166 than other evapotranspiration schemes, because this question is beyond the scope of the current paper.

167

## 168 **2.2. Mathematical framework for predicting aggregation bias**

### 169 *Nonlinear averaging using second-order Taylor expansions*

170 ET is a nonlinear function of its drivers. An intrinsic property of any nonlinear function is that the average of  
171 the function will not equal the function evaluated at the average inputs (e.g., Rastetter et al., 1992; Giorgi and  
172 Avissar, 1997; [Rouholahnejad Freund and Kirchner, 2017](#)). Thus averaging over sub-grid heterogeneity in ET  
173 drivers, as large-scale land surface models do, would be expected to lead to biased ET estimates, even if the  
174 underlying equations were exactly correct. For an ET function of three variables, namely  $R_n$ ,  $w_w$ , and  $T$ , the  
175 mean of the ET function, in terms of the function's value at the mean of its inputs, can be approximated by the  
176 second-order Taylor series expansion of the ET function (Eq. 6):

$$177 \quad \begin{aligned} \overline{ET} &\approx \widehat{ET} + \frac{1}{2} \left[ \frac{\partial^2 ET}{\partial R_n^2} \text{Var}(R_n) + \frac{\partial^2 ET}{\partial w_w^2} \text{Var}(w_w) + \frac{\partial^2 ET}{\partial T^2} \text{Var}(T) \right] \\ &\quad + \frac{\partial^2 ET}{\partial R_n \partial T} \text{Cov}(R_n, T) + \frac{\partial^2 ET}{\partial R_n \partial w_w} \text{Cov}(R_n, w_w) + \frac{\partial^2 ET}{\partial w_w \partial T} \text{Cov}(w_w, T), \end{aligned} \quad (7)$$

178 where  $\overline{ET}$  is the estimate of the true average of the nonlinear ET function over its variable inputs,  $\widehat{ET}$  is the ET  
179 function evaluated at its mean inputs, and the derivatives are understood to be evaluated at the mean values  
180 of the variables ( $\overline{R_n}, \overline{w_w}, \overline{T}$ ) [and multiplied by the corresponding variances and covariances among finer-](#)

181 [resolution input data](#). For the specific case of the GLEAM model, [the ET function is evaluated at its mean inputs](#)  
 182 [\( \$\widehat{ET}\$ \) and](#) these derivatives are derived analytically from the ET function described by Eq. 6, directly yielding the  
 183 following expressions:

$$184 \quad \widehat{ET} = [-4\bar{w}_w^2 + 4.8\bar{w}_w - 0.44] * 0.02905 * \frac{a e^{b\bar{T}}}{a e^{b\bar{T}} + 0.073} \bar{R}_n, \quad (8)$$

$$185 \quad \frac{\partial^2 ET}{\partial R_n^2} = 0, \quad (9)$$

$$186 \quad \frac{\partial^2 ET}{\partial w_w^2} = [-8] * 0.02905 * \frac{\Delta}{\Delta + \gamma} R_n \quad (w_{wp} \leq w_w \leq w_c), \quad (10a)$$

$$187 \quad \frac{\partial^2 ET}{\partial w_w^2} = 0 \quad (w_w < w_{wp}, \quad w_w > w_c), \quad (10b)$$

$$188 \quad \frac{\partial^2 ET}{\partial T^2} = [-4w_w^2 + 4.8w_w - 0.44] * 0.02905 * R_n * b^2 * \frac{\gamma^2 \Delta - \gamma \Delta^2}{(\gamma + \Delta)^3}, \quad (11)$$

$$189 \quad \frac{\partial^2 ET}{\partial R_n \partial T} = [-4w_w^2 + 4.8w_w - 0.44] * 0.02905 * \frac{\Delta}{\Delta + \gamma} * \frac{b\gamma}{\Delta + \gamma}, \quad (12)$$

$$190 \quad \frac{\partial^2 ET}{\partial R_n \partial w_w} = [-8w_w + 4.8] * 0.02905 * \frac{\Delta}{\Delta + \gamma} \quad (w_{wp} \leq w_w \leq w_c), \quad (13a)$$

$$191 \quad \frac{\partial^2 ET}{\partial R_n \partial w_w} = 0 \quad (w_w < w_{wp}, \quad w_w > w_c), \quad (13b)$$

$$192 \quad \frac{\partial^2 ET}{\partial w_w \partial T} = [-8w_w + 4.8] * 0.02905 * \frac{\Delta}{\Delta + \gamma} * \frac{b\gamma}{\Delta + \gamma} * R_n \quad (w_{wp} \leq w_w \leq w_c), \quad \text{and} \quad (14a)$$

$$193 \quad \frac{\partial^2 ET}{\partial w_w \partial T} = 0 \quad (w_w < w_{wp}, \quad w_w > w_c), \quad (14b)$$

194 where  $\Delta$  depends on temperature as described in Eq. (4). The difference between the average of the functions  
 195 ( $\widehat{ET}$ ) and the function of the averages ( $\overline{ET}$ ), or, equivalently, the sum of all the other terms in Eq. (7),  
 196 represents the aggregation bias. The magnitude of this bias can be calculated by combining Eqs. 7-14 with  
 197 estimates of the variances and covariances of the input variables. [Note that the interception term in equation](#)  
 198 [6 is dropped out from the derivatives as the interception loss in GLEAM is a linear function of amount of](#)  
 199 [rainfall necessary to saturate the canopy and therefore has negligible effect when averaged.](#)

200  
 201 The approach outlined in Eq. (7) is general and could be extended to other land surface modeling schemes.  
 202 The partial derivatives in Eqs. (8-14), of course, are specific to the GLEAM equations; for other models they  
 203 would differ. More complex land surface model algorithms may not have such simple analytical derivatives; in  
 204 that case, the derivatives can be evaluated numerically.

205

### 206 **2.3. Sub-grid heterogeneity and aggregation bias in ET estimates across Switzerland**

207 Drivers of ET (i.e., soil moisture, net radiation, and temperature) can be highly heterogeneous within the grid  
 208 cells of typical ESMs. Soil moisture can show pronounced spatial variability, especially in areas where surface  
 209 roughness, porosity, and permeability vary by orders of magnitude across a variety of length scales (Giorgi and  
 210 Avissar, 1997). Temperature and incoming radiation vary significantly with season, elevation, altitude, and

211 albedo. Switzerland, for example, shows strong local variations in average annual temperature, soil moisture  
212 content, net radiation, and albedo (Fig. 1; albedo values in Fig. S1).

213

214 We quantified how averaging over spatial (and temporal) heterogeneities of ET drivers affects estimated ET at  
215 several grid scales across Switzerland, as an example case for which high-resolution data are available. Our  
216 analysis is based on 500-m input data of temperature (interpolation of MeteoSwiss data after Viviroli et al.,  
217 2009), net radiation (Viviroli et al., 2009), and soil moisture (simulations from the hydrological model PREVAH,  
218 Brunner et al., 2019; Speich et al., 2015; Orth et al., 2015; Zappa et al., 2003) at daily time steps for the 2004  
219 growing season. Although our soil moisture data are derived from model simulations whose accuracy is  
220 difficult to assess due to the scarcity of real-world soil moisture measurements, for our purposes all that is  
221 necessary is that the simulated values exhibit realistically complex spatial variability.

222

223 We used the GLEAM equations, as outlined in Sect. 2, to calculate ET for each day at the 500-m resolution of  
224 these input data. We use these 500-m ET estimates as virtual "truth" for the purpose of our analysis, because  
225 our goal is not to determine whether GLEAM estimates of ET are accurate (compared to direct measurements,  
226 for example), but rather to quantify how spatial aggregation affects them.

227

228 To quantify how spatial aggregation affects model estimates of ET, we calculated ET over larger spatial scales  
229 in two different ways. First, we averaged the 500-m ET estimates over 1/32, 1/16, 1/8, 0.25, 0.5, 0.75, 1, and 2-  
230 degree grid cells across Switzerland, to represent the "true" average ET at those grid scales. Second, we  
231 averaged the 500-m input data (of temperature, soil moisture, and net radiation) over the same grid cells, and  
232 then used these grid-cell-averaged input data in the GLEAM equations to calculate the modeled coarse-  
233 resolution ET at each grid scale. The deviation of the modeled coarse-resolution ET from the "true" average ET  
234 measures the aggregation bias. Because this numerical experiment uses the same model equations, based on  
235 the same underlying data, for the ET calculations at each spatial resolution, it isolates spatial aggregation as  
236 the only possible cause of the difference between the "true" average ET ( $\overline{ET}$  in Eq. 7) and the coarse-resolution  
237 modeled ET ( $\widehat{ET}$  in Eq. 7) at each grid scale.

238

239 Figure 2a shows that the ET aggregation bias varies considerably across Switzerland, and also varies  
240 considerably with grid scale. The average aggregation bias is higher at coarser grid scales, averaging 21.410%  
241 ~~at 2-degree grid resolution and 16.8% at and~~ -1-degree grid resolution across all of Switzerland (calculated as  
242 the median of the daily aggregation biases over the growing season; Fig. 2a). Smaller grid scales typically  
243 exhibit smaller aggregation biases (averaging 74% at 1/16-degree grid resolution across all of Switzerland  
244 calculated as the median of the daily aggregation biases over the growing season) because they typically  
245 average over less spatial heterogeneity, but even at the smallest grid scales, aggregation biases can locally  
246 ~~exceed reach~~ 6840%, as indicated by the ~~red grid cells~~ scatter plot in Fig. ~~2a3~~. These figures are medians of the  
247 daily aggregation biases for over the entire growing season of 2004; the aggregation biases of two randomly

248 selected days (May 31<sup>st</sup> and July 21<sup>st</sup>, 2004) at several spatial scales [are lead to](#) much larger overestimation of  
 249 ET in parts of southern Switzerland (Figs. S2, S3).

250

251 Using our 500-m input data, we can test how well Eq. (7) estimates the difference between the "true" average  
 252 ET and the coarse-resolution modeled ET at each grid scale. We used Eqs. (8-14) to calculate the partial  
 253 derivatives of the GLEAM equations for each grid cell and time step, using the grid-cell averaged values of the  
 254 input data. We then multiplied these derivatives by the corresponding variances and covariances among the  
 255 500-m input data to obtain bias estimates via Eq. (15) for each grid cell and time step:

$$256 \quad \text{Bias} = \widehat{\text{ET}} - \overline{\text{ET}} \approx -\frac{1}{2} \left[ \frac{\partial^2 \text{ET}}{\partial R_n^2} \text{Var}(R_n) + \frac{\partial^2 \text{ET}}{\partial w_w^2} \text{Var}(w_w) + \frac{\partial^2 \text{ET}}{\partial T^2} \text{Var}(T) \right] \\
 - \frac{\partial^2 \text{ET}}{\partial R_n \partial T} \text{Cov}(R_n, T) - \frac{\partial^2 \text{ET}}{\partial R_n \partial w_w} \text{Cov}(R_n, w_w) - \frac{\partial^2 \text{ET}}{\partial w_w \partial T} \text{Cov}(w_w, T), \quad (15)$$

257 where  $\overline{\text{ET}}$  is the true average ET at some grid resolution,  $\widehat{\text{ET}}$  is the modeled coarse-resolution ET at the same  
 258 spatial scale, the right-hand side is the Taylor expansion estimate of the aggregation bias. We then compared  
 259 these estimated biases against the "true" aggregation biases (the difference between the "true" average ET  
 260 and the coarse-resolution modeled ET) in the numerical experiment described above. The true bias, in other  
 261 words, is  $\widehat{\text{ET}} - \overline{\text{ET}}$  in Eq. (15), and the estimated bias is the Taylor approximation on the right-hand side.

262

263 Figure 2b shows that the aggregation bias estimated by Eq. (15) is generally similar, in both overall magnitude  
 264 and spatial distribution, to the "true" aggregation biases calculated by the numerical experiment. This  
 265 comparison is shown more explicitly in Fig. 3, in which the estimated aggregation bias is compared with the  
 266 "true" aggregation bias for each grid cell at each grid scale. Figures 2 and 3 show that Eq. (15) is generally a  
 267 good predictor of aggregation bias. Both the estimated aggregation biases (Fig. 2) and the "true" aggregation  
 268 biases are markedly higher in regions of greater topographic complexity (Fig. S4).

269

## 270 **2.4. Correcting for aggregation bias**

### 271 **2.4.1. Identifying drivers of aggregation bias**

272 The Taylor expansion in Eq. (15) not only allows one to quantify the aggregation bias; it also allows one to  
 273 quantify the relative importance of the three input variables (net radiation, soil moisture, and temperature) as  
 274 drivers of that bias. Each of the terms in Eq. (15) combines a variance or covariance that expresses how  
 275 variable the input data are, and a second derivative that expresses how sensitive the average ET is to that  
 276 variability. Each of these terms – a derivative multiplied by a variance or covariance – has the same units as ET,  
 277 and thus they can be directly compared to one another.

278

279 Table 1 shows each of the aggregation bias terms, calculated over all of Switzerland for the two randomly  
 280 chosen days mentioned in Sect. [4-2.3](#) (May 31<sup>st</sup> and July 21<sup>st</sup>, 2004). For these two example days, the  
 281 aggregation bias is clearly dominated by a single term, associated with the variance of soil moisture. The  
 282 variance in net radiation ( $R_n$ ) creates no aggregation bias, because GLEAM ET is a linear function of  $R_n$ ; thus

283 positive and negative deviations from average  $Rn$  will increase and decrease ET by exactly offsetting amounts.  
284 Similarly, the variance in temperature ( $T$ ) also results in little aggregation bias, because GLEAM ET increases  
285 nearly linearly with  $T$  across a wide range of temperature. The covariance terms similarly lead to little  
286 aggregation bias. By contrast, the strong curvature in the quadratic dependence of ET on soil moisture (Eq. 6)  
287 implies that positive and negative deviations from mean soil moisture will not have offsetting ET effects, and  
288 thus that spatial heterogeneity in soil moisture can significantly alter average ET.

289

#### 290 2.4.2. Correcting for aggregation bias using sub-grid closure relationships

291 The Taylor expansion framework in Eq. (7) can be used not only to diagnose aggregation bias, but also to  
292 estimate sub-grid closure relationships that correct for the effects of small-scale heterogeneity. The variance  
293 and covariance terms in Eq. (7) express how sub-grid heterogeneity affects average ET at the grid scale,  
294 implying that these aggregation bias estimates could be used to improve grid-scale ET estimates, without  
295 explicitly modeling ET at high resolutions. This approach could be particularly useful in land surface algorithms  
296 that are part of coarser-resolution Earth system models; in such cases it may be much more efficient to  
297 evaluate Eqs. 7-14 at the coarse grid resolution than to directly evaluate the underlying ET model, Eq. 6, at  
298 high resolution. The Taylor expansion approach could also be attractive where we lack spatially explicit high-  
299 resolution maps of the ET drivers, but where their variances and covariances can nonetheless be estimated  
300 from other sources (such as from the variability of topography, mapped soil units, remote sensing data, etc.).

301

302 It is beyond our scope here to construct such variance and covariance estimates, but we can illustrate how  
303 they could potentially be used. The solid red symbols in Fig. 4 show the relationships between "true" average  
304 ET and modeled grid-cell-averaged ET, for each grid cell (and one example day, ~~July~~ ~~May~~ ~~21~~ ~~31~~<sup>st</sup>, 2004) at  
305 several different grid scales. For comparison, the open grey symbols in Fig. 4 show average ET estimated by the  
306 Taylor expansion approach of Eq. (7), which corrects for sub-grid heterogeneity effects using only grid-cell-  
307 averaged estimates of the ET drivers and their small-scale variances and covariances.

308

309 The heterogeneity-corrected ET estimates shown by the open symbols in Fig. 4 cluster much closer to the 1:1  
310 line than the modeled grid-cell-averaged ET values shown by the solid red symbols, suggesting that the Taylor  
311 expansion approach may substantially improve estimates of grid-cell-averaged ET. Real-world results may be  
312 less clear than those shown in Fig. 4, because the heterogeneity-corrected ET estimates (the open symbols in  
313 Fig. 4) are calculated using exact values for the variances and covariances of the ET drivers within each grid  
314 cell, and in real-world cases these variances and covariances will not be known precisely. Figure 4 nonetheless  
315 demonstrates the potential value of knowing, or being able to estimate, those variances and covariances.  
316 Efforts to determine those variances and covariances can be focused on the terms that matter the most, if one  
317 can identify the main drivers of aggregation bias using the methods described in Sect. ~~5-12.2~~ above.



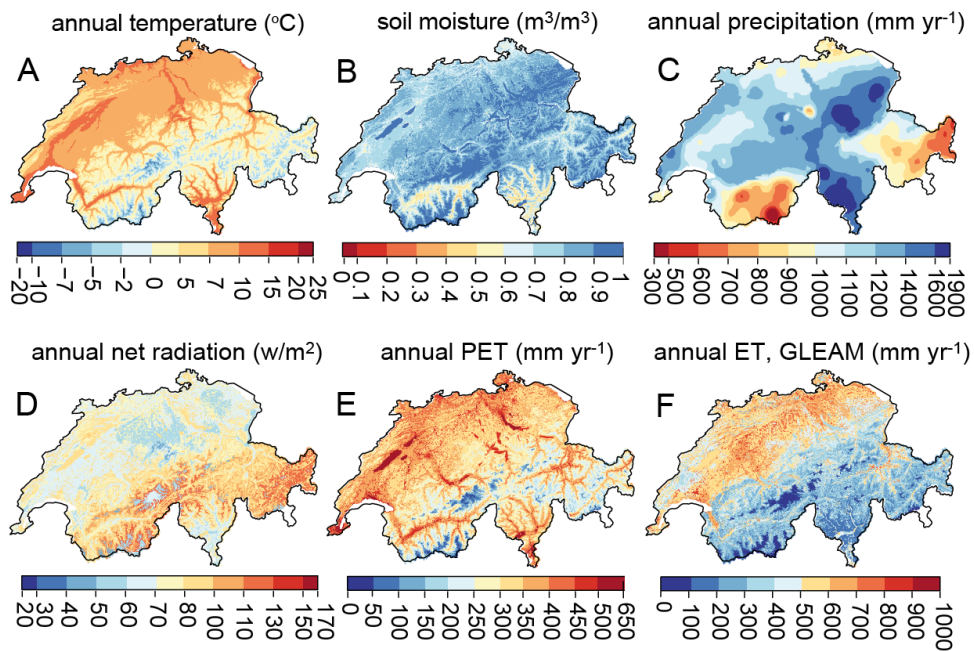
318  
 319  
 320  
 321  
 322  
 323  
 324  
 325  
 326  
 327  
 328  
 329  
 330

Table 1. Relative importance of different ET drivers in aggregation bias estimates (different terms in Eq. 15). Values are calculated for all of Switzerland for the two randomly chosen days (May 31st and July 21st, 2004). The aggregation bias is dominated by the term associated with the variance of soil moisture for these two example days.

|             | $\widehat{ET}$<br>mm d <sup>-1</sup> | $\overline{ET}$<br>mm d <sup>-1</sup> | Bias<br>%                | Contribution<br>of $Var(R_n)$<br>term in %<br>aggregation<br>bias (%)                   | Contribution<br>of $Var(w_w)$<br>term in %<br>aggregation<br>bias (%)                   | Contribution<br>of $Var(T)$<br>term in %<br>aggregation<br>bias (%)                 | Contribution<br>of $Cov(R_n, T)$<br>term in %<br>aggregation<br>bias (%)                | Contribution<br>of $Cov(R_n, w_w)$<br>term in %<br>aggregation<br>bias (%)                  | Contribution<br>of $Cov(R_n, w_w)$<br>term in %<br>aggregation<br>bias (%)              |
|-------------|--------------------------------------|---------------------------------------|--------------------------|---|---|---|---|---|---|
| Calculation | (Eq. 8)                              | (Eq. 7)                               | (Eq. 15)                 | $\frac{1}{2} \frac{\partial^2 ET}{\partial R_n^2} Var(R_n)$<br>( $\widehat{ET}$ . Bias) | $\frac{1}{2} \frac{\partial^2 ET}{\partial w_w^2} Var(w_w)$<br>( $\widehat{ET}$ . Bias) | $\frac{1}{2} \frac{\partial^2 ET}{\partial T^2} Var(T)$<br>( $\widehat{ET}$ . Bias) | $\frac{\partial^2 ET}{\partial R_n \partial T} Cov(R_n, T)$<br>( $\widehat{ET}$ . Bias) | $\frac{\partial^2 ET}{\partial R_n \partial w_w} Cov(R_n, w_w)$<br>( $\widehat{ET}$ . Bias) | $\frac{\partial^2 ET}{\partial w_w \partial T} Cov(w_w, T)$<br>( $\widehat{ET}$ . Bias) |
| 31.05.2004  | <del>2.6582.3</del>                  | <del>1.6361.8</del><br>9              | <del>38.43</del><br>21.7 | 0   | 97.9481.65  | 0.0490  | 0.481.05  | 0.222.80  | 1.3214.41   |
| 21.07.2004  | 2.3811                               | 1.6851.8<br>4                         | 29.16<br>14.84           | 0   | 94.6783.35  | 1.052.34  | 3.036.56  | 0.331.84  | 0.926.01  |

331  
 332

333  
334

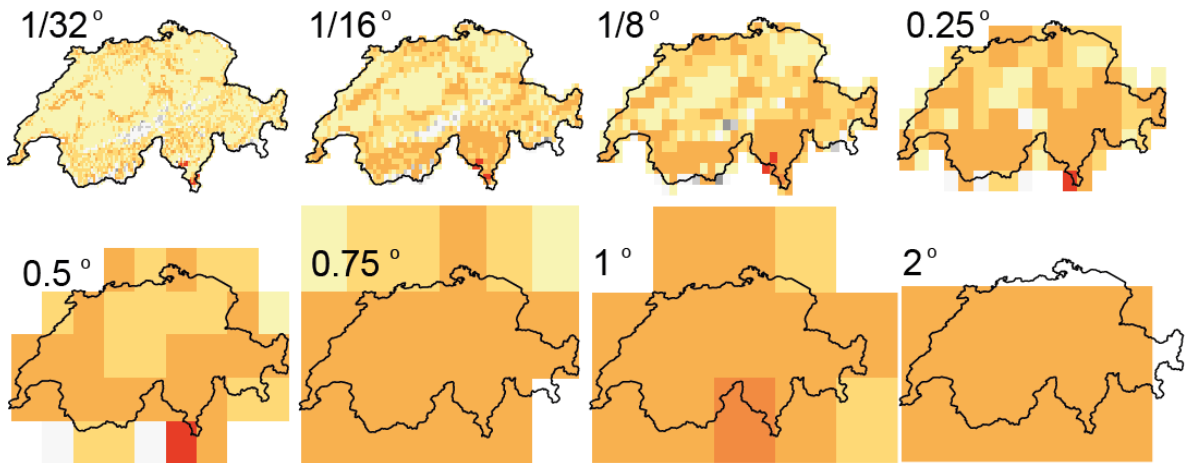


335

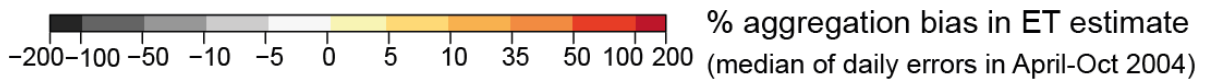
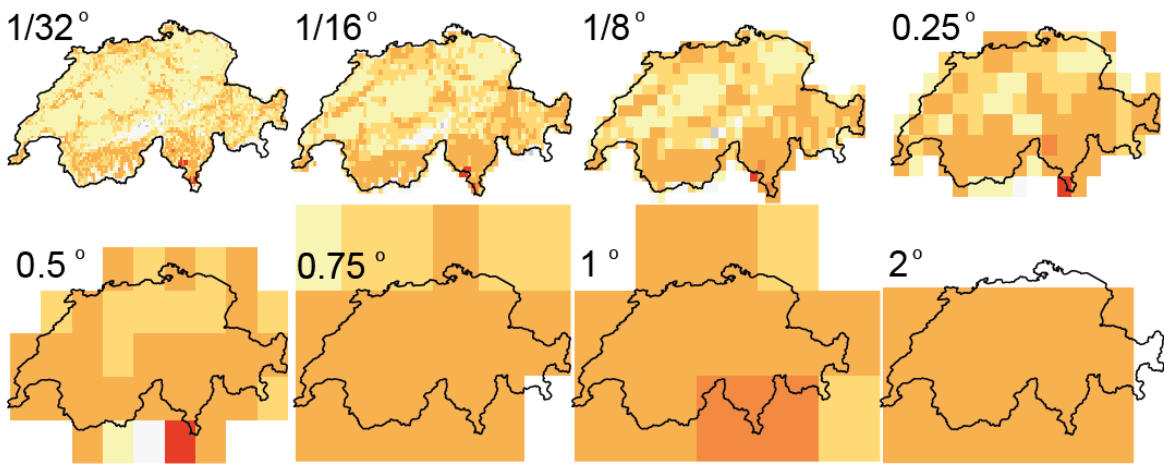
336 Figure 1. Spatial distribution of input data for the year 2004 at 500-m resolution: Annual mean (A) temperature  
337 (°C), (B) soil moisture ( $\text{m}^3 \text{m}^{-3}$ , simulated by the PREVAH hydrological model), (C) precipitation ( $\text{mm yr}^{-1}$ ), (D)  
338 net radiation ( $\text{W m}^{-2}$ ), (E) potential evapotranspiration (PET,  $\text{mm yr}^{-1}$ ) using the Priestley-Taylor equation (Eq.  
339 3), and (F) evapotranspiration (ET,  $\text{mm yr}^{-1}$ ) using the approach used in the GLEAM model (Eq. 1). See Table. S1  
340 for references.

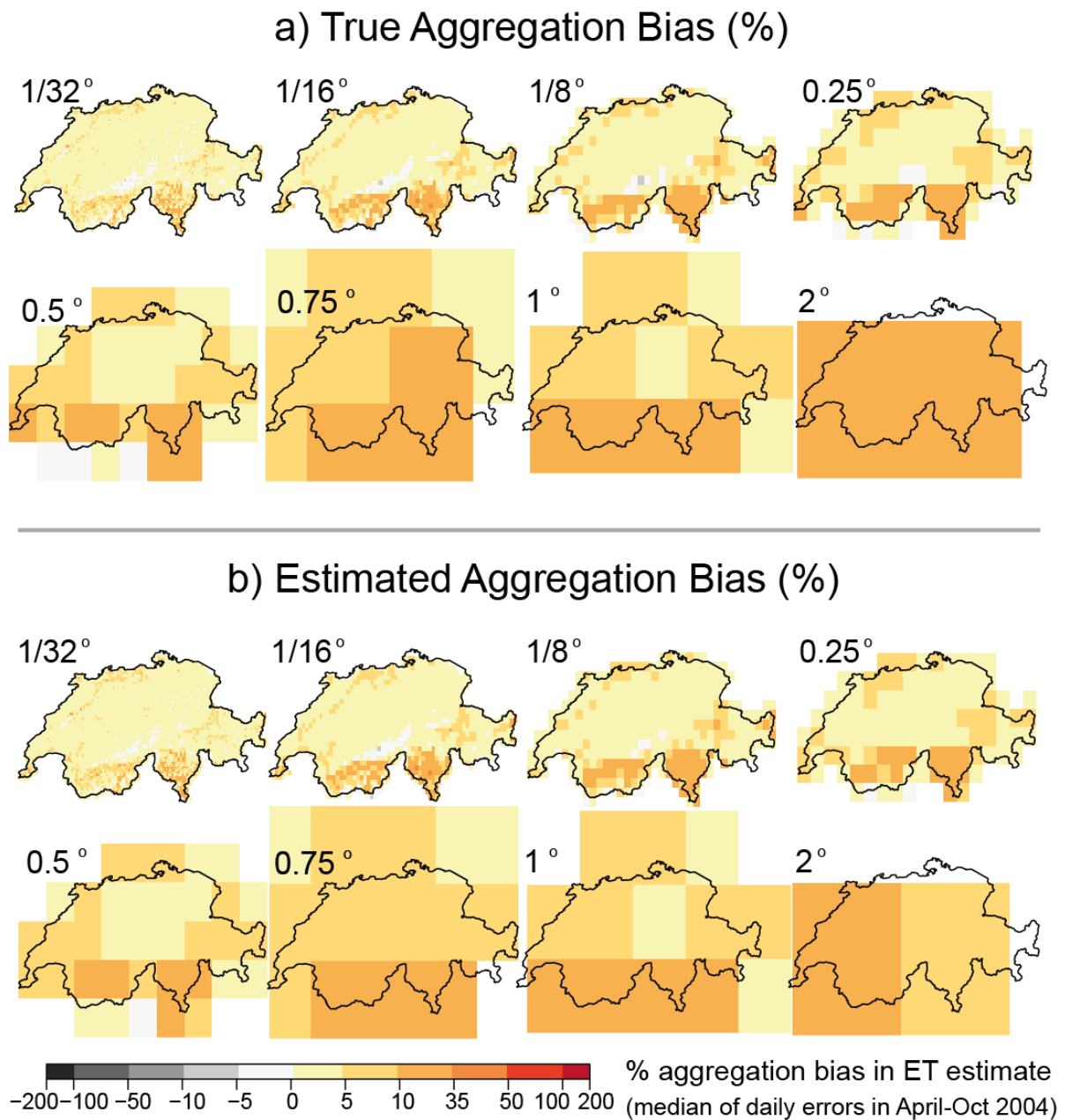
341

### a) True Aggregation Bias (%)



### b) Estimated Aggregation Bias (%)

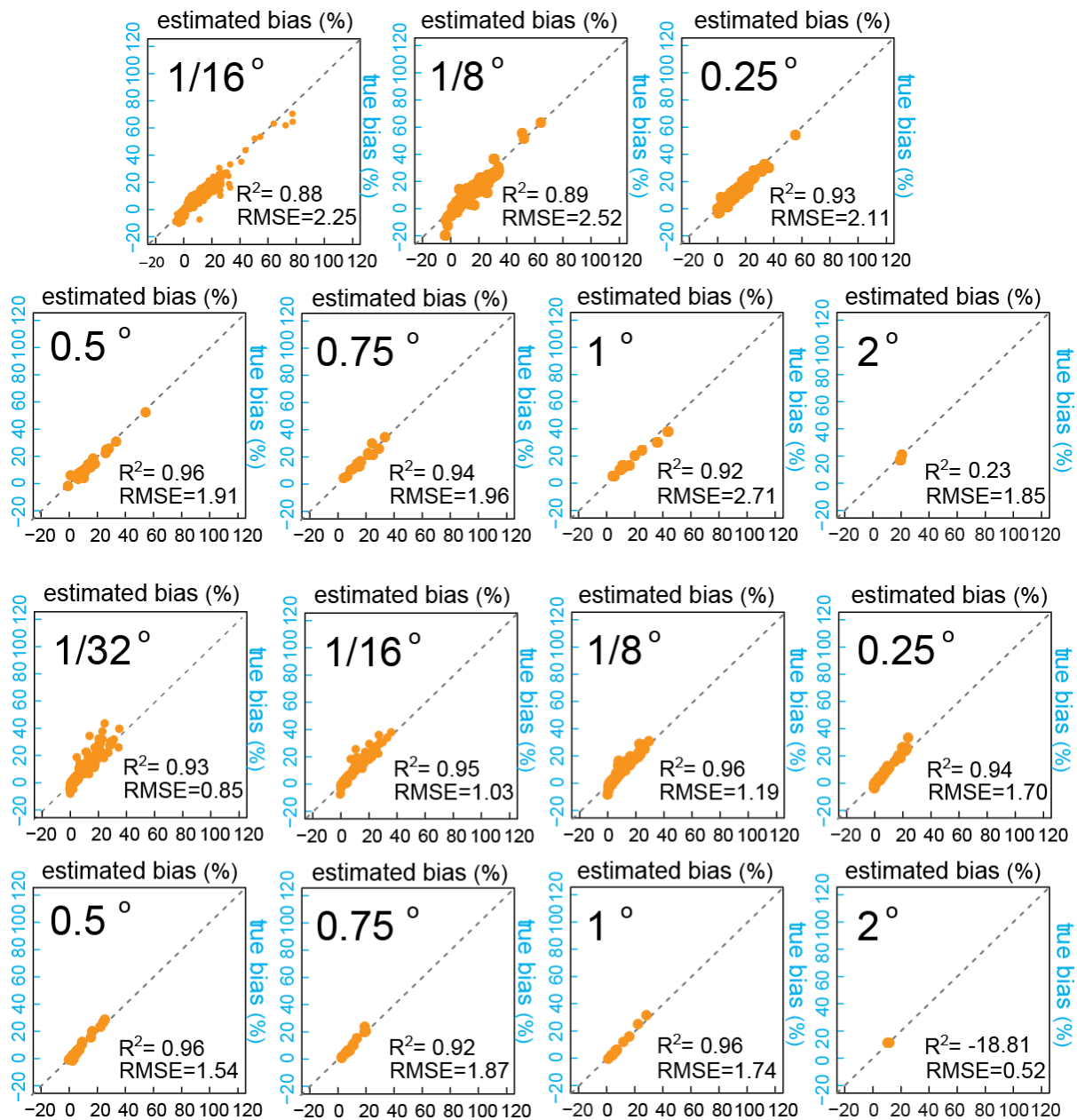




344

345 Figure 2. a) “True” aggregation bias in ET, as calculated by averaging the 500-m resolution ET estimates using  
 346 fine-resolution input data in Eq. 6, over 1/32, 1/16, 1/8, 0.25, 0.5, 0.75, 1, and 2-degree grid cells across  
 347 Switzerland. b) Aggregation bias in ET, as estimated by Eq. 7 from grid-cell averaged temperature ( $^{\circ}\text{C}$ ), soil  
 348 moisture ( $w_w$ ), net radiation ( $R_n$ ), their variances at each grid scale, and the covariances of all pairs of variables  
 349 using the 500-m input data. At finer grid scales, the aggregation bias is more localized, and smaller on average.  
 350 Across Switzerland as a whole, average aggregation bias becomes smaller as grid scales become finer, but  
 351 never disappears completely.

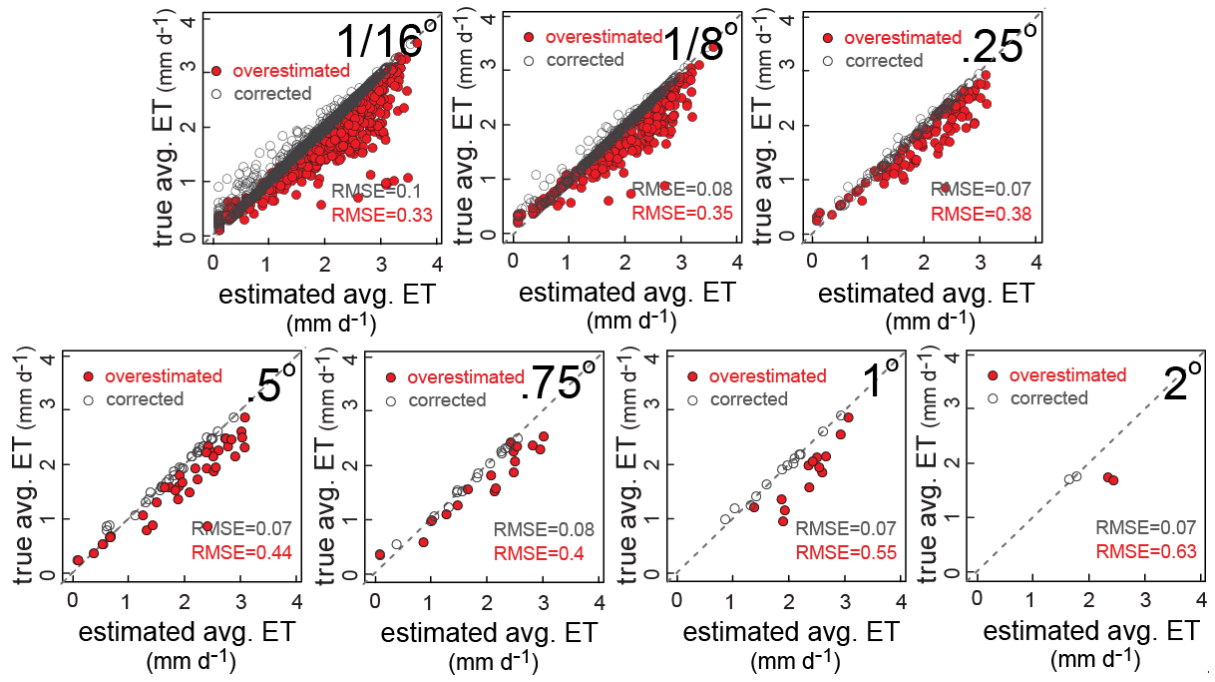
352



353

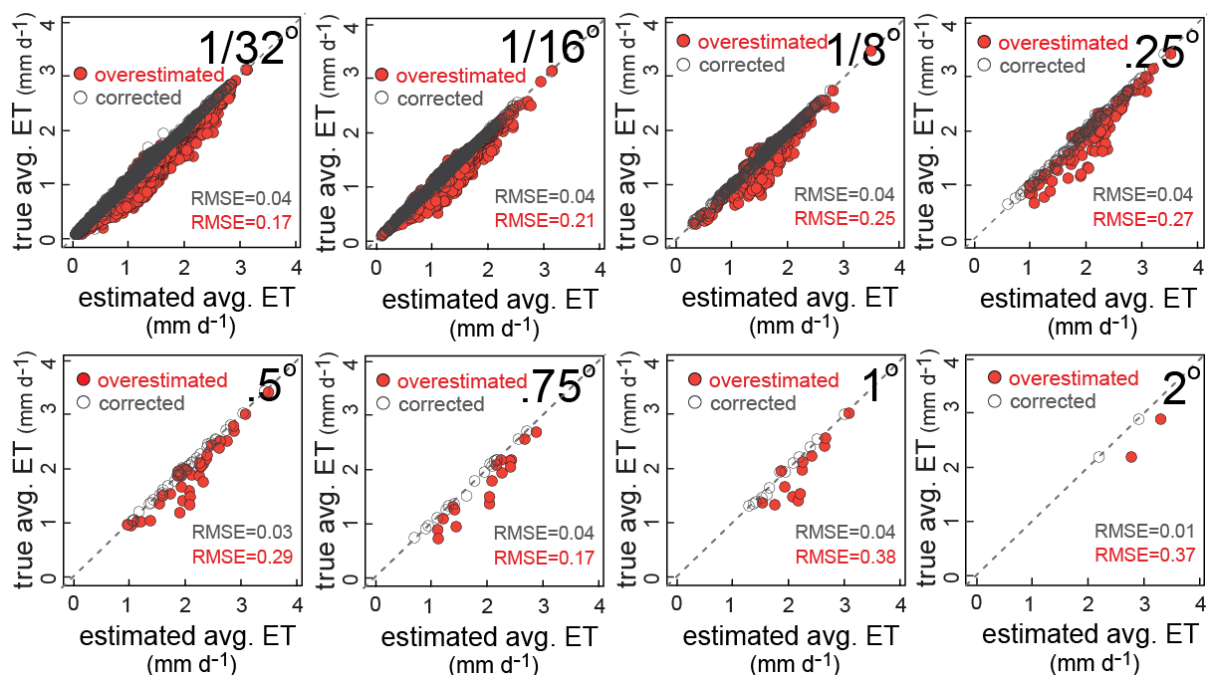
354

355 Figure 3. Daily estimated aggregation bias in ET estimates (% , median of daily biases in Apr.-Oct. 2004) versus  
 356 daily true aggregation bias in ET estimates (% , median of daily biases in Apr.-Oct. 2004) at several spatial  
 357 scales. Estimated aggregation biases are calculated using Eq. 7. True aggregation biases are calculated as  
 358 differences between the finer resolution ET estimates from finer resolution input data, averaged over several  
 359 spatial scales (average of functions) and ET values calculated from average inputs at each spatial scale  
 360 (function of averages). The coefficients of determination ( $R^2$ ) between the true and estimated aggregation  
 361 biases verify the reliability of the Taylor expansion method and Eq. 7 as estimates of the aggregation bias.



362

363



365

366 Figure 4. Daily estimated ET rates versus “true” average ET at each grid cell at several different grid scales  
 367 (example day, [July May 21<sup>st</sup>31<sup>st</sup>](#), 2004). The solid red symbols demonstrate the relationships between “true”  
 368 average ET calculated using fine-resolution data at each grid cell and modeled grid-cell-averaged ET using grid-  
 369 cell-averaged inputs in Eq.8, for each grid cell at several different grid scales (overestimated). For comparison,  
 370 the open symbols show true average versus average ET estimated by the Taylor expansion approach of Eq. (7),  
 371 which corrects for sub-grid heterogeneity effects using only grid-cell-averaged estimates of the ET drivers and  
 372 their small-scale variances and covariances (heterogeneity-corrected ET estimates, corrected).

373

### 374 3. Discussion

375 Averaging over spatially heterogeneous ET drivers leads to substantial aggregation biases in ET flux estimates  
 376 from a typical mechanistic large-scale land surface model. This aggregation bias arises from the inherent  
 377 nonlinearities in evapotranspiration processes, coupled with the inherent spatial heterogeneity in the driving  
 378 factors. The joint effects of these nonlinearities and heterogeneities can be estimated using second-order  
 379 Taylor expansions of the governing equations. Using Switzerland as a test case, we have shown that median  
 380 aggregation biases of 10-35% are common, even at grid scales substantially smaller than those typically used in  
 381 land surface models (Fig. 2). These biases can be much larger for individual days (Figs. S2 and S3)- [and](#)  
 382 [potentially These biases can](#) have substantial consequences for water and energy flux estimates in land surface  
 383 models and consequently for temperature predictions in coupled models. The overestimated evaporative  
 384 fluxes would lead to overestimated latent heat fluxes and underestimated sensible heat fluxes, and thus  
 385 potentially to underestimates of expected temperature increases in a changing climate. Unrealistically high  
 386 evaporation estimates lead to cooler modeled temperatures and wetter modeled climates. Correcting for the

387 aggregation bias in ET fluxes would lead to reduced evaporative cooling and increased atmospheric heating via  
388 sensible heat flux.

389

390 In coupled Earth system models, ET fluxes influence how surface temperature, net radiation, and soil moisture  
391 evolve through time, and thus influence future values of ET. The analyses shown in Figs. 2-4 are based on static  
392 values for each day, and thus do not account for the propagation of aggregation biases forward through time.  
393 Estimating the consequences of aggregation biases for dynamic modeling would require fully coupled Earth  
394 system model simulations rather than the single ET algorithm analyzed here. In a dynamic model, the Taylor  
395 expansion approach can potentially be used to correct for aggregation biases in each time step, using  
396 statistical models for the variances and covariances of the ET drivers. Thus, estimating aggregation biases in a  
397 dynamic model would not require explicitly simulating sub-grid heterogeneity at every time step. Correcting  
398 for aggregation biases at each modeling time step would prevent them from propagating further into future  
399 time steps, or into the partitioning of future water and energy fluxes at the land surface. The present paper  
400 does not illustrate this dynamic correction for aggregation biases, but establishes the theoretical framework  
401 for it.

402

403 The purpose of our analysis was to demonstrate how aggregation bias due to spatial heterogeneity can be  
404 quantified (Sects. [2.23-42.3](#)), how its dominant drivers can be identified (Sect. [5-12.4.1](#)), and how its effects  
405 can be efficiently corrected for, using sub-grid closure relationships (Sect. [5-22.4.2](#)). For this demonstration, we  
406 chose GLEAM as an illustrative example, and Switzerland as a topographically complex case study where high-  
407 resolution data on the ET drivers are available. Applications of this approach to more complex land surface  
408 models may require calculating the necessary derivatives (see Eq. 7) numerically rather than analytically, and  
409 applications where high-resolution data are unavailable may require statistically estimating the variances and  
410 covariances among the drivers of ET, based on their relationships with topography, soil types, land cover, etc.  
411 Using the approach outlined here, one can account for the effects of sub-grid heterogeneity without explicitly  
412 modeling ET at fine spatial resolution, which could be impractical due to computational costs, or impossible  
413 due to a lack of fine-resolution input data.

414

415 In our analysis, spatial heterogeneity in soil moisture emerged as the dominant driver of aggregation bias in ET  
416 estimates. Particularly if this result can also be confirmed in other regions and climates, it points to the  
417 importance of improving our understanding of spatial patterns of soil moisture and what controls them. The  
418 lower topographic curvature of coarsely gridded landscapes can lead models to predict higher soil moisture at  
419 coarser grid scales (Kuo et al., 1999); higher soil moisture at larger grid scales would lead to even higher  
420 modeled values of ET, beyond the effects of the aggregation biases analyzed here. Soil moisture may also be  
421 substantially influenced by lateral subsurface transfers of water, which are ignored in our analysis and are also



422 ignored by many land surface models. Overlooking lateral transfers could potentially bias ET estimates in large-  
423 scale land surface models (Fan et al., 2019), but this is beyond the scope of the present study.

424

425

426 **Acknowledgements**

427 We thank Prof. Ying Fan Reinfelder for numerous insightful discussions and for helpful comments on the  
428 manuscript. E.R.F. acknowledges support from the Swiss National Science Foundation (SNSF) under Grant No.  
429 P2EZP2\_162279.

430 **Data Availability Statement**

431 We will upload the source data for this study to a FAIR repository and provide the URL with the final version of  
432 the paper.

433

434

435 **References**

- 436 Beven, K. J., and ~~H. L. Cloke, H. L.~~: Comment on “Hyperresolution global land surface modeling: Meeting a  
437 grand challenge for monitoring Earth's terrestrial water” by Eric F. Wood et al., Water Resour. Res., 48,  
438 W01801, <https://doi.org/doi:10.1029/2011WR010982>, 2012.
- 439 Beven, K. J.: The holy grail of scientific hydrology:  $Q_t=H(SR)A$  as closure, Hydrol. Earth Syst. Sci., 10, 609–618,  
440 <https://doi.org/10.5194/hess-10-609-2006>, 2006.
- 441 Boone, A., and O. J. Wetzel: A simple scheme for modeling sub-grid soil texture variability for use in an  
442 atmospheric climate model, Journal of the Meteorological Society of Japan, 77(1), 317–333,  
443 [https://doi.org/10.2151/jmsj1965.77.1B\\_317](https://doi.org/10.2151/jmsj1965.77.1B_317), 1998.
- 444 Brunner, M. I., ~~K. Liechti, K., & M. Zappa, M.~~: Extremeness of recent drought events in Switzerland:  
445 dependence on variable and return period choice, Natural Hazards and Earth System Science, 19(10), 2311–  
446 2323, <https://doi.org/10.5194/nhess-19-2311-2019>, 2019, 2019.
- 447 Brunt, D.: Physical and dynamical meteorology, 2<sup>nd</sup> ed., Univ. Press, Cambridge. 428 pp, 1952.
- 448 Brutsaert, W.: Evaporation into the atmosphere, ISBN 978-90-481-8365-4, DOI [https://doi.org/10.1007/978-](https://doi.org/10.1007/978-94-017-1497-6)  
449 94-017-1497-6, 1984.
- 450 BFS, Die Bodennutzung der Schweiz: Arealstatistik 1979/85, Bundesamt fuer Statistik, Bern, 1995.
- 451 Budyko, M. I.: Climate and life, Academic, New York, 1974.
- 452 Bundesamt für Landestopographie: Digitales Höhenmodell RIMINI, Wabern,  
453 [https://www.bfs.admin.ch/bfs/de/home/dienstleistungen/geostat/geodaten-](https://www.bfs.admin.ch/bfs/de/home/dienstleistungen/geostat/geodaten-bundesstatistik/topografie.assetdetail.230215.html)  
454 [bundesstatistik/topografie.assetdetail.230215.html](https://www.bfs.admin.ch/bfs/de/home/dienstleistungen/geostat/geodaten-bundesstatistik/topografie.assetdetail.230215.html), 1991.
- 455 El Maayar, M. , and J. M. Chen: Spatial scaling of evapotranspiration as affected by heterogeneities in  
456 vegetation, topography, and soil texture, Remote Sensing of Environment, 102, 33–51,  
457 <https://doi.org/10.1016/j.rse.2006.01.017>, 2006.
- 458 Ershadi A., M. F. McCabe, J. P. Evans, and J. P. Walker: Effects of spatial aggregation on the multi-scale  
459 estimation of evapotranspiration, Remote Sensing of Environment, 131, 51–62,  
460 <http://dx.doi.org/10.1016/j.rse.2012.12.007>, 2013.
- 461 Fan, Y., M. Clark, D. M. Lawrence, S. Swenson, L. E. Band, S. L. Brantley, P. D. Brooks, W. E. Dietrich, A. Flores,  
462 G. Grant, J. W. Kirchner, D. S. Mackay, J. J. McDonnell, P. C. D. Milly, P. L. Sullivan, C. Tague, H. Ajami, N.  
463 Chaney, A. Hartmann, P. Hazenberg, J. McNamara, J. Pelletier, J. Perket, E. Rouholahnejad-Freund, T. Wagener,  
464 X. Zeng, E. Beighley, J. Buzan, M. Huang, B. Livneh, B. P. Mohanty, B. Nijssen, M. Safeeq, C. Shen, W. van  
465 Verseveld, and J. Volk, D. Yamazaki: Hillslope hydrology in global change research and Earth system modeling,  
466 Water Resources Research, 55, <https://doi.org/doi:10.1029/2018WR023903>, 2019.
- 467 Gash, J. H. C.: an analytical model of rainfall interception by forests, Q. J. R. Meteorol. Soc. 105 (433), 43–55,  
468 <https://doi.org/10.1002/qj.49710544304>, 1979.

469 Giorgi, F.: [An Approach for the Representation of Surface Heterogeneity in Land Surface Models. Part I:](#)  
470 [Theoretical Framework](#), Mon. Wea. Rev., 125, 1885–1899, <https://doi.org/10.1175/1520->  
471 [0493\(1997\)125<1885:AAFTRO>2.0.CO;2](https://doi.org/10.1175/1520-0493(1997)125<1885:AAFTRO>2.0.CO;2), 1997.

472 Giorgi, F., and R. Avissar: Representation of heterogeneity effects in Earth system modeling: Experience from  
473 land surface modeling, Rev. Geophys., 35, 413–437, <https://doi.org/10.1029/97RG01754>, 1997.

474 Greve, P., B. Orlowsky, B. Mueller, J. Sheffield, M. Reichstein, and S. I. Seneviratne: Global assessment of  
475 trends in wetting and drying over land, Nature Geoscience, 7: 716, 2014.

476 Hong, S. H., J. M. H. Hendrickx, and B. Borchers: Up-scaling of SEBAL derived evapotranspiration maps from  
477 Landsat (30 m) to MODIS (250 m) scale, Journal of Hydrology, 370, 122–138,  
478 <https://doi.org/10.1016/j.jhydrol.2009.03.002>, 2009.

479 Huang, X., A. M. Rhoades, P. A. Ullrich, and C. M. Zarzycki: An evaluation of the variable-resolution- CESM for  
480 modeling California’s climate, J. Adv. Model. Earth Syst., 8, 345–369, doi:10.1002/2015MS000559, 2016.

481 Jasechko, S., Z. D. Sharp, J. J. Gibson, S. J. Birks, Y. Yi, and P. J. Fawcett: Terrestrial water fluxes dominated by  
482 transpiration, Nature, 496: 347, <https://doi.org/10.1890/ES13-00391.1>, 2013.

483 Kuo, W. L., T. S. Steenhuis, C. E. T. S., McCulloch, C. E., C. L. Mohler, C. L., D. A. Weinstein, D. A., S. D. DeGloria,  
484 S. D., and D. P. Swaney, D. P.: Effect of grid size on runoff and soil moisture for a variable-source-area  
485 hydrology model, Water Resour. Res., 35(11), 3419–3428, <https://doi.org/10.1029/1999WR900183>,  
486 1999.

487 Martens, B., D. G. Miralles, H. Lievens, R. van der Schalie, R. A. M. de Jeu, D. Fernández-Prieto, H. E. Beck, W. A.  
488 Dorigo, and N. E. C. Verhoest: GLEAM v3: satellite-based land evaporation and root-zone soil moisture,  
489 Geosci. Model Dev. 10(5): 1903–1925, <https://doi.org/10.5194/gmd-10-1903-2017>, 2017.

490 McCabe M., and E. Wood: Scale influences on the remote estimation of evapotranspiration using multiple  
491 satellite sensors, Remote Sensing of Environment 105, 271–285, <https://doi.org/10.1016/j.rse.2006.07.006>,  
492 2006.

493 Miralles, D. G., T. R. H. Holmes, R. A. M. De Jeu, J. H. Gash, A. G. C. A. Meesters, and A. J. Dolman: Global land-  
494 surface evaporation estimated from satellite-based observations, Hydrol. Earth Syst. Sci. 15(2): 453–469,  
495 <https://doi.org/10.5194/hess-15-453-2011>, 2011.

496 Miralles, D. G., A. J. Teuling, C. C. van Heerwaarden, and J. Vilà-Guerau de Arellano: Mega-heatwave  
497 temperatures due to combined soil desiccation and atmospheric heat accumulation, Nature Geosci, 7(5):  
498 345–349, <https://doi.org/10.1038/NGEO2141>, 2014.

499 Miralles, D. G., M. J. van den Berg, J. H. Gash, R. M. Parinussa, R. A. M. de Jeu, H. E. Beck, T. R. H. Holmes, C.  
500 Jiménez, N. E. C. Verhoest, W. A. Dorigo, A. J. Teuling, and A. Johannes Dolman: El Niño–La Niña cycle and  
501 recent trends in continental evaporation, Nature Climate Change, 4: 122,  
502 <https://doi.org/10.1038/NCLIMATE2068>, 2013.

503 Monteith, J. L., and M. H. Unsworth: Principles of Environmental Physics, Edward Arnold, London, 1990.

504 Monteith, J. L.: Evaporation and environment, the state of and movement of water in living organisms,  
505 Proceeding of Soc. for Exp. Biol., 19, 205–234, doi:10.1002/qj.49710745102, 1965.

506 Mueller, B., M. Hirschi, C. Jimenez, P. Ciais, P. A. Dirmeyer, A. J. Dolman, J. B. Fisher, M. Jung, F. Ludwig, F.  
507 Maignan, D. G. Miralles, M. F. McCabe, M. Reichstein, J. Sheffield, K. Wang, E. F. Wood, Y. Zhang, and S. I.  
508 Seneviratne: Benchmark products for land evapotranspiration: LandFlux-EVAL multi-data set synthesis, Hydrol.  
509 Earth Syst. Sci. 17(10): 3707–3720, <https://doi.org/10.5194/hess-17-3707-2013>, 2013.

510 Murray, F. W.: On the computation of saturation vapor pressure, J. Appl. Meteor. 6: 203–204,  
511 [https://doi.org/10.1175/1520-0450\(1967\)006<0203:OTCOSV>2.0.CO;2](https://doi.org/10.1175/1520-0450(1967)006<0203:OTCOSV>2.0.CO;2), 1967.

512 Orth, R., M. Staudinger, S. I. M., Seneviratne, S. I., J. Seibert, J., & M. Zappa, M.: Does model performance  
513 improve with complexity? A case study with three hydrological models, Journal of Hydrology, 523, 147–159,  
514 <https://doi.org/10.1016/j.jhydrol.2015.01.044>, 2015.

515 Penman, H. L.: Natural evaporation from open water, bare soil, and grass, Proc. Roy. Soc. London A193,  
516 120–146, 1948.

517 Priestley, C. H. B., and R. J. Taylor, R. J.: On the assessment of surface heat flux and evaporation using large-  
518 scale parameters, Monthly Weather Review, 100, 81–92, [https://doi.org/10.1175/1520-0493\(1972\)100<0081:otaosh>2.3.co;2](https://doi.org/10.1175/1520-0493(1972)100<0081:otaosh>2.3.co;2), 1972.

520 Rauscher, S. A., E. Coppola, C. Piani, and F. Giorgi: Resolution effects on regional climate model simulations of  
521 seasonal precipitation over Europe, Clim. Dyn., 35(4), 685–711, <https://doi.org/10.1007/s00382-009-0607-7>,  
522 2010.

523 Ringler, T., L. Ju, and M. Gunzburger: A multiresolution method for climate system modeling: Application of  
524 spherical centroidal Voronoi tessellations, Ocean Dyn., 58(5–6), 475–498, <https://doi.org/10.1007/s10236-008-0157-2>, 2008.

526 Rouholahnejad Freund, E., and J. W. Kirchner: A Budyko framework for estimating how spatial heterogeneity  
527 and lateral moisture redistribution affect average evapotranspiration rates as seen from the atmosphere,  
528 Hydrology and Earth System Sciences, 21(1), 217–233, <https://doi.org/10.5194/hess-21-217-2017>, 2017.

529 Rouholahnejad Freund, E., Y. Fan, and J. W. Kirchner: Global assessment of how averaging over spatial  
530 heterogeneity in precipitation and potential evapotranspiration affects modeled evapotranspiration rates,  
531 [Hydrol. Earth Syst. Sci., 24, 1927–1938](https://doi.org/10.5194/hess-24-1927-2020) ~~Hydrol. Earth Syst. Sci. Discuss.,~~ <https://doi.org/10.5194/hess-24-1927-2020>, 2020. <https://doi.org/10.5194/hess-2019-103>, in review, 2019.

533

534 Seneviratne, S. I., T. Corti, E. L. Davin, M. Hirschi, E. B. Jaeger, I. Lehner, B., Orlowsky, and A. J. Teuling, et al.:  
535 Investigating soil moisture–climate interactions in a changing climate: A review, Earth-Science Reviews 99(3–  
536 4): 125–161, <https://doi.org/10.1016/j.earscirev.2010.02.004>, 2010.

537 Shrestha, P., M. Sulis, C. ~~Simmer~~Simmer, and S. Kollet: Impacts of grid resolution on surface energy fluxes  
538 simulated with an integrated surface-groundwater flow model, Hydrol. Earth Syst. Sci. 19(10): 4317–4326,  
539 <https://doi.org/10.5194/hess-19-4317-2015>, 2015.

540 Shrestha, P., M. Sulis, C. ~~Simmer~~Simmer, and S. Kollet: Effects of horizontal grid resolution on evapotranspiration  
541 partitioning using TerrSysMP, Journal of Hydrology, 557: 910–915,  
542 <https://doi.org/10.1016/j.jhydrol.2018.01.024>, 2018.

543 Skamarock, W. C., J. B. Klemp, M. G. Duda, L. D. Fowler, S.-H. Park, and T. D. Ringler, A multiscale  
544 nonhydrostatic atmospheric model using centroidal Voronoi tessellations and C-grid staggering, Mon. Weather  
545 Rev., 140(9), 3090–3105, <https://doi.org/10.1175/MWR-D-11-00215.1>, 2012.

546 Speich, M. J. R., ~~L. Bernhard~~L. Bernhard, ~~A. J. Teuling~~A. J. Teuling, ~~& and M. Zappa~~M. Zappa, M.: Application of bivariate mapping for  
547 hydrological classification and analysis of temporal change and scale effects in Switzerland–, Journal of  
548 Hydrology, 523, 804–821, <https://doi.org/10.1016/j.jhydrol.2015.01.086>, 2015.

549 Stanghellini, C., Transpiration of Greenhouse Crops. PhD thesis, Wageningen University, Wageningen, The  
550 Netherlands, 1987.

551 Tetens, O., ~~Über~~Über einige meteorologische Begriffe. z. Geophys. 6:297–309, 1930.

552 Viviroli, D., ~~M. Zappa~~M. Zappa, ~~M. J. Gurtz~~M. J. Gurtz, ~~& and R. Weingartner~~R. Weingartner, R.: An introduction to the hydrological modelling  
553 system PREVAH and its pre- and post-processing-tools–, Environmental Modelling and Software, 24(10), 1209–  
554 1222, <https://doi.org/10.1016/j.envsoft.2009.04.001>, 2009.

555 Zappa, M. and ~~J. Gurtz~~J. Gurtz, J.: Simulation of soil moisture and evapotranspiration in a soil profile during the 1999  
556 MAP-Riviera Campaign, Hydrol. Earth Syst. Sci., 7, 903–919, <https://doi.org/10.5194/hess-7-903-2003>, 2003.

557 Zarzycki, C. M., M. N. Levy, C. Jablonowski, J. R. Overfelt, M. A. Taylor, and P. A. Ullrich–, Aquaplanet  
558 experiments using CAM’s variable-resolution dynamical core, J. Clim., 27(14), 5481–5503,  
559 <https://doi.org/10.1175/JCLI-D-14-00004.1>, 2014.

560

561